INFLUENCE OF CREPE STRUCTURE ON TENSILE PROPERTIES OF TISSUE PAPER

Shubham Agarwal, Prabhat Srivastava, Sheldon I. Green and A. Srikantha Phani

Department of Mechanical Engineering, The University of British Columbia, Vancouver, Canada

ABSTRACT

Tissue is a low-density paper product distinguished by a microscale crepe structure. We investigate the relationship between the macroscale tissue tensile response and crepe structure. We propose a parameter called the Crepe Index (CI) that can be measured from edge images of the creped sheet. Crepe Index correlates very well with the measured tensile failure strain ("stretch"), but its correlation with the measured initial elastic stiffness is unclear. A discrete elastoplastic model (DEM) is developed to explain the experimental results and understand the nonlinearity in the tensile curve. The model accounts for both material nonlinearity through a bilinear elastoplastic constitutive law for the sheet material, and the geometric nonlinearity arising from large deformations. The creped sheet is idealized as a triangular wave of prescribed wavelength and waveheight, with nonlinear bending and stretching effects. The model results show that the tensile response is governed by both the nonlinearity of the sheet material (fibre network) and crepe structure (geometry). The yielding in stretching and bending gives rise to an inflection in the tensile response. It is found that the initial stiffness depends not only on CI, but also on parameters such as sheet-thickness to crepe-wavelength ratio, and stiffness of sheet material after creping. Thus, the variability in above parameters can be one of the reason for unclear correlation between

measured initial stiffness and CI. For CI range of tested commercial tissues, both experiments and model show that stretch varies linearly with CI, with an almost unity slope and a positive intercept (i.e, stretch> CI). Thus, the overall stretch of creped tissue is a sum of CI and network stretching.

1 INTRODUCTION

Tissue papers are lightweight materials with applications in hygiene, packaging, and engineering. Grammage for tissue papers lies below 25 g/m^2; a typical office paper in contrast has a grammage of 80 g/m^2. There are several processes to manufacture tissue papers such as, through air drying (TAD), new tissue technology (NTT), and advanced tissue molding system (ATMOS). However, owing to low cost and high production speed, a process called dry-creping is often employed by tissue manufacturers [1]. This manufacturing process includes four major steps: forming, pressing, drying, and creping. A mat of wet wood fibres is formed in the forming section, pressed, and then transferred to a rotating heated drum with pre-applied adhesive (the Yankee dryer). Typical Yankee surface speeds are around 20 m/s. After having dried to a solid content (SC) of around 95%, the dried mat is scraped off from the Yankee using a Creping blade. Figure 1(a) shows a schematic of the drying section and creping. The web-blade interaction is shown schematically in Figure 1(b). The violent interaction of web with the blade gives rise to periodic delamination and buckling of sheet, resulting a folded microstructure in the machine direction (MD); the *crepe structure* [2–4]. In addition to tissue papers, folded structures may also be found on different scales in other materials, such as nano-folded graphene sheets [5,6], folded plant leaves [7,8], and mountain structures (orogeny) [9]. Engineered mechanical metamaterials are known to exhibit nonlinear mechanical properties owing to their complex geometry [10]. Although the actual crepe structure is not exactly periodic due to factors such as wiremark, inhomogeneity in web properties and adhesion, a dominant creping wavelength can be identified. In addition to folding in the MD, the sheet can simultaneously *de-densify* in the ZD due to inter-fibre bond rupture. In summary, creping disrupts the fibre network of the original sheet, resulting in its folding, foreshortening, and de-densification. Relative to an uncreped sheet, a creped sheet shows increased failure strain ("stretch"), bulk, and softness and a concomitant tensile degradation [11–13]. In a commercial tissue production process, tissue is converted after creping (embossing, printing), which further modifies its properties; however, in this study, we will focus on the properties of unconverted tissue paper to understand the effect of creping. Edge-on images of unconverted creped tissues (Figure 1(c)) show that its structure can lie broadly in
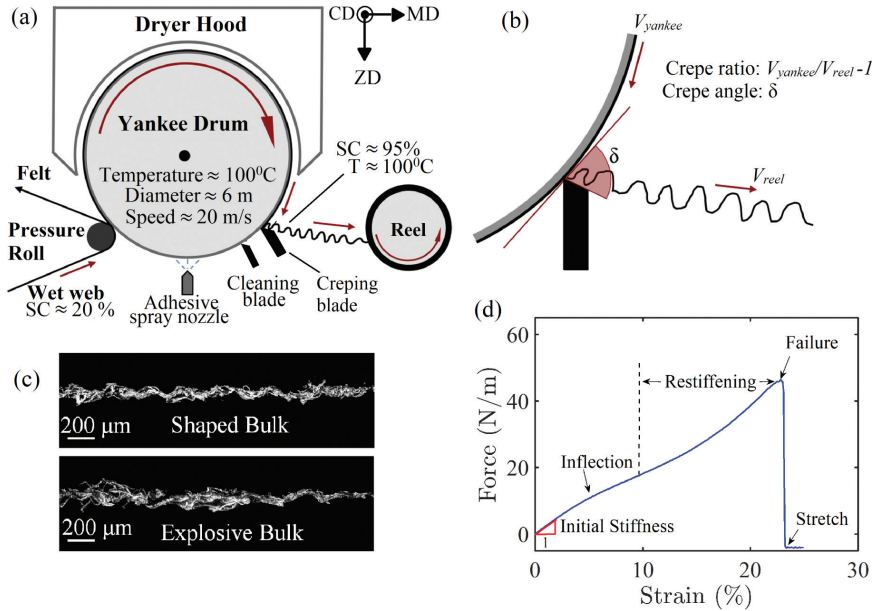
Figure 1. (a) A schematic of the creping process. SC is the solid content of the web. MD is the machine direction and ZD is the direction perpendicular to the plane of the sheet. The orthogonal direction, out of the plane, is the cross direction, CD; (b) Magnified view of the web-blade contact area. The creping angle δ is defined as the angle between the tangent to the Yankee surface and the blade surface; (c) Edge images of unconverted commercial tissue grades demonstrating shaped and explosive bulk; (d) A typical MD tensile response of a commercial tissue paper, y-axis represents force per unit sample width. Images (a,b) are adapted from [14].

two regimes: shaped bulk and explosive bulk. In the former, one can easily identify a crepe structure and the associated dominant wavelength and amplitude. However, in the latter massive inter-fibre separation is also observed.

The tensile response of uncreped handsheets is known to be nonlinear due several micro-scale parameters, such as fibre plasticity, non-affine network deformation, inter-fibre bonds, and sheet microstructure [15–20]. Thus, creped paper can be thought as a complex metamaterial having nonlinearity due to geometry (crepe structure) as well as the base material (fibre network). Figure 1(d) shows a typical uniaxial tensile response of an unconverted commercial tissue paper [21]. The nonlinear response begins with an initial stiffness (E_0). At an intermediate strain around 5% the response softens, following an inflection it stiffens again around a strain of 10%, and finally fails around a strain between 20% and 25%.

Shubham Agarwal, Prabhat Srivastava, Sheldon I. Green and A. Srikantha Phani

The overall tensile response is dependent on the fibre properties, network structure (anisotropy, formation), and the folded structure imparted due to creping. The aim of this work is to understand the tensile response nonlinearity and the effect of crepe structure on stretch and initial stiffness.

To understand the effect of crepe structure on tensile response, its quantification is necessary. The literature on the structural quantification of creped sheets is limited. Traditionally, Crepe Ratio is used in industry to quantify the extent of creping, or the degree of foreshortening of sheet during creping. As mentioned in Figure 1(b), Crepe Ratio (CR) is defined in terms of surface speeds of Yankee and reel as $CR = V_{yankee}/V_{reel} - 1$. However, there is no published data on the correlation between CR and sheet foreshortening. Das [22] calculated Crepe Frequency (number of folds per unit machine direction length of unstretched tissue paper) for commercial tissues using a surface imaging technique. However, such surface imaging provides little information on the amplitude of creped folds. Therefore, a new experimental procedure is required to capture details of the crepe structure more comprehensively.

Pan et al.[14] applied one-dimensional particle dynamics model to study the effect of creping parameters on the tensile response on an elastoplastic creped sheet and found a tensile response that is qualitatively similar to that of experiments. Pan observed that the stretch is directly correlated with the ratio of crepe amplitude and crepe wavelength [23]. An inextensible bending model (IBM) by Vandenberghe et al. treats the crêpe sheet as a triangular wave of rigid links, connected through elastic-perfectly plastic bending springs [24]. They show that the stress-strain inflection appears at the onset of yielding in the bending springs. Since, their model does not consider the extensibility of links, the contribution from the stretching mode of deformation is absent. The structural stiffness in case of IBM approaches infinity due to singularity at zero Crepe Index, which is not physical. The assumption that the tensile response of creped tissue is entirely dominated by bending is questionable, as the experimental tensile tests of tissue paper by Das [21] and Srivastava [25] show evidence of both structural unfolding and network stretching.

The above studies underscore the importance of sheet structure and material nonlinearity on the tensile properties of the tissue. The influence of crepe structure and material nonlinearity on the tensile response of tissue is not understood in detail. The objective of this paper is to answer the following questions:

- How can we quantify the degree of folding in a tissue paper?
- What can be a macroscale origin of the nonlinear evolution of the tensile response of a crepedtissue?
- How does the degree of folding in the creped tissue affect its initial stiffness and stretch?

The structure of the paper is as follows, section 2 discusses the Crepe Index parameter for structural quantification, experimental method for Crepe Index calculation, and tensile tests. Later in this section, experimental results showing the correlation of stretch and initial stiffness with Crepe Index are discussed. The tensile response nonlinearity and the effect of Crepe Index on the tensile properties are explained using a discrete elastoplastic model (DEM) for a creped sheet. The modelling method and results are discussed in section 3. Finally, the article closes with conclusions and future work.

2 EXPERIMENTS

In this section, we will first define the parameter called Crepe Index for structural quantification. Experimental methods for Crepe Index measurement and tensile test are then discussed. Finally, the experimental results are presented, discussing the variation of stretch and initial stiffness with the Crepe Index.

2.1 Crepe Index

Recalling Figure 1(c), consider a MD-ZD slice through a creped sheet, as shown schematically in Figure 2. We define the centerline of the sheet as the locus of the midpoint of top and bottom boundary in ZD. Thus, for a given horizontal sample length L_s, one can calculate the contour length L_c for the centerline. A measure for the degree of folding of the sheet can be expressed by a geometrical parameter called the Crepe Index (CI), which can be defined as:
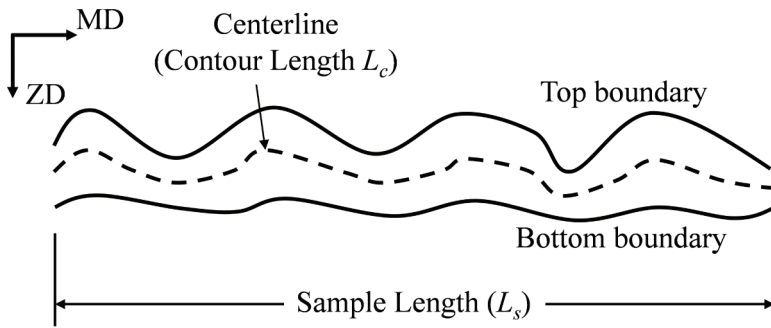
$$CI = \frac{L_c}{L_s} - 1. \tag{1}$$

Figure 2. Schematic of a MD-ZD slice of a tissue paper showing top boundary, bottom boundary, and centerline. The contour length of the centerline is L_c for a sample of length L_s in MD.

From the above definition, one can interpret Crepe Index as the strain required to completely unfold a folded structure, assuming no change in total length L_c of structure (inextensible unfolding). Thus, CI gives a geometrical contribution of stretch. However, stretch for real tissue is a combination of CI and strain due to network stretching. The comparison between CI and actual stretch values will be discussed in later sections. Though similar, CI is fundamentally different from Curl Index [26]. Curl Index is a 3D quantity defined for slender objects like fibres and hair, where the difference between segment and contour length can be due to stretching, bending, as well as twisting. However, Crepe Index is a 2D quantity defined for a sheet, in which the difference between segment and contour length is expected due to bending and stretching of the sheet. Another index with similar definition is Tortuosity, which is defined for a curve as the arc-chord ratio (L_c/L_s). Tortuosity is often used to describe diffusion and fluid flow in porous media, such as soil and snow [27,28]. Thus, CI can also be defined as Tortuosity of a 2D curve minus 1.

2.2 Experimental Method

2.2.1 Focus Stacking Based Micro-imaging Technique

Creping produces micro folds (wavelength $\approx 300~\mu m$) in sheets. Such features can reasonably be imaged at sufficiently high magnification ($\geq 10X$). In optical imaging, a major problem encountered at such high magnification is the shallow depth of field. This challenge can be overcome using focus stacking. We use this principle to capture the edge images of the tissue sample. More details about the experimental setup can be found in [25], a brief summary of the setup is presented as follows. The tissue sample is held horizontally with one edge facing the camera. The sample is tensioned as per ISO 12625-4 [29], to remove any slack. The edge of the sample is illuminated using diffused sources of light. The imaging setup, light and specimen are surrounded by a cage with black sheets to eliminate the effects of ambient light and air movement. The whole system is operated remotely. To capture an image, a 24 megapixels DSLR camera is mounted on a focus stacking rail (step resolution of 1 μm). Extension bellows, tube lens (focal length = 200 mm), extension tubes, and a 10X plan floor infinity-corrected microscope objective lens (focal length 20 mm and working distance of 17.5 mm) are attached to the camera. A circular lens support is used to hold the lens horizontally and prevent its bending. The distance between the objective lens and tube lens is 110 mm and that between the camera sensor plane and tube lens is ≈ 150 mm. The entire setup is mounted on a stable platform to avoid effects due to vibrations.

To image the edge of a tissue sample, several images are obtained at increments of 1 μm out of the plane of focus of the lens, with focal-plane movement provided by the focus stacking rail. Each separate image is then de-hazed and has its texture

and clarity enhanced. Following above preprocessing, all of the images are stacked using a commercial focus stacking software, which identifies the most focused portion of individual images and stacks them to form a single focused image. Once stacked, the image is masked from the background to remove any noise. More details about the imaging process can be found in [25].

2.2.2 Tensile Tests

The initial stiffness and stretch of six commercial tissue grades are experimentally measured using the INSTRON 5969 universal tester. The test follows the ISO-12625-4 standard [29], a sample with 25.4 mm width and 100 mm gauge length is pulled at a rate of 50 mm/min. Inertial effects on the load-extension plots are negligible at this extension rate. The resulting load-extension data are converted to force/width vs strain ($f_w - \varepsilon$) plots. To calculate f_w, the total load (f) is divided by sample width ($= 25.4mm$); strain is obtained by dividing the displacement by the sample gauge length ($= 100mm$). From the obtained tensile curve, initial stiffness and stretch are calculated. As defined in Figure 1(d), stretch is the failure-strain, and initial stiffness (E_0) is the initial slope of the tensile curve. We estimate the initial stiffness by measuring the slope of the experimentally obtained tensile curve between 0% and 2% strain.

2.3 Experimental Results

We employ the edge imaging technique explained in section 2.2.1 to calculate the Crepe Index (CI) of different commercial tissue grades. The grades differ in furnish, grammage, caliper and drying conditions. Using multiple edge images ($n \approx 18$), we estimate the mean and the standard error of CI for each tissue grade. Edge images of two grades (A and B) having the same furnish are identified in Figure 3(a). Relevant parameters for these two grades are summarized in Table A.1 in Appendix A. Through a visual inspection it can be observed that the structure of tissue A (CI = 10.1±0.6 %) has smaller amplitude and large wavelength (or, more flat), as compared to that of tissue B (CI = 15.3±0.7 %). Thus, a tissue with higher CI has higher degree of folding, as suggested by equation 1. The tensile responses for grades A and B are shown in Figure 3(b). As manifested, grade B (with higher CI) has softer response with higher stretch.

To study the dependence of stretch and initial stiffness of tissue on the Crepe Index, the values measured from uniaxial tensile tests for different grades. The mean and standard error in tensile properties are calculated though multiple tensile tests of each grade (n ≈ 10). As seen in Figure 3(c), despite of the variability in furnish and machine conditions, a very good correlation is observed between the stretch and CI for all grades. The slope of the stretch-CI line is almost
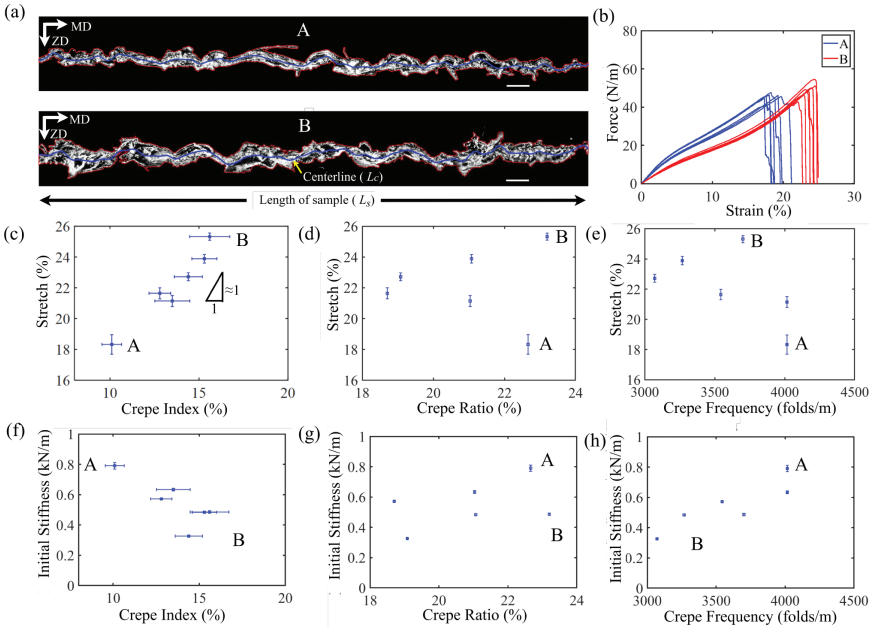
Figure 3. Initial stiffness and stretch of unconverted creped basesheets produced using different fibers and under different operating conditions: (a) Selected edge images generated through focus stacking with centerline (blue curve), top and bottom boundaries (red curves). Scalebar represents a length of $100\mu m$. (b) Tensile responses of grades A and B. Dependence of stretch on: (c) Crepe Index, (d) Crepe Ratio, and (e) Crepe Frequency. Dependence of initial stiffness on: (f) Crepe Index, (g) Crepe Ratio, and (h) Crepe Frequency. Points A and B correspond to the grades shown in Figure 3 (a). The horizontal and vertical error bars are standard errors of respective quantities.

1, and the measured stretch values are higher than the CI (positive intercept). The linear dependence of stretch on CI can be explained by the geometric argument presented while defining CI in section 2.1. The observation that the measured stretch values are higher than the CI implies that the overall stretch is a sum of CI effects and the strain due to network stretching. We will verify this observation later in this paper through modelling. Figures 3 (d) and (e) compare stretch with Crepe Ratio (CR) and Crepe Frequency (CF) respectively. The comparisons show that that stretch has a poor correlation with CR and CF. Thus, out of the above three parameters, the correlation of stretch is most reasonable with the CI. Also, the disparity among Figures 3(c) and (d) show that CI and CR are two different quantities, although dividing the numerator and denominator in CI expression with time yields the expression of CR. Above disparity suggest that

creping is not just an inextensible buckling process, which is assumed while arguing for the equality the two expressions.

The initial stiffness of creped sheet shows an unclear correlation with CI and CR, as shown in figures 3(f) and (g). A fairly good correlation between initial stiffness and CF can be observed in 3(h). However, as the CF increases the fold count increases (more wavy structure)), thus, the initial stiffness is expected to reduce due to more bending effects, but opposite is being observed. One possible reason for the above discrepancy is that CF does not include the amplitude information which will also govern the initial stiffness. For instance, comparing grades A and B, grade A has higher CF (lower fold wavelength) but lower CI, which suggests that that it has a lower fold amplitude, thus increasing the initial stiffness. Therefore, CF alone does not give the full information about the degree of folding in a creped sheet, thus the associated tensile properties. In summary, neither of CI, CR, and CF shows a clear and explainable correlation with the initial stiffness.

The natural question which arises is whether we should expect any dependence of initial stiffness with a geometric parameter like CI. As mentioned earlier, the initial stiffness of a creped sheet is expected to depend on material properties of base sheet (fibre properties) and geometry (crepe structure, thickness). Thus, for the fixed material properties, one should expect a correlation between initial stiffness and CI. In the experimental data shown in Figure 3(f), grades A and B share the same furnish, and a reduction in initial stiffness with CI is observed. However, the furnish for rest of the grades is different, that may be one reason why initial stiffness data seems uncorrelated with CI. We will investigate the dependence of initial stiffness on CI through modelling in the next section, and explain the potential reasons for the inconclusive experimental correlation.

3 MODELLING

To understand the tensile response nonlinearity and explain the experimental observations, we propose a discrete elastoplastic model (DEM). In the following subsections we discuss the method and assumptions used for modelling. Model results are first compared with the geometry based and inextensible bending model (IBM) [24]. Later, the model results are discussed and linked with experimental observations.

3.1 Method: Discrete Elastoplastic Model (DEM)

Figure 3(a) is an edge view showing crepe structure of a commercial tissue grade, imaged using focus stacking imaging technique. Especially in the shaped bulk regime, one can identify a wave pattern with a dominant wavelength or crepe

wavelength, and a dominant wave height or caliper. To model the mechanics of unfolding during uniaxial tensile test, we approximate crepe structure as a triangular wave of dominant wavelength λ_0, wave height A_0, and an effective sheet-thickness t. Note that, in the model, t is the thickness of an approximated continuum sheet, thus can be different than that of real sheet due to its porous structure. Figure 4(a) shows one wavelength of such an approximated wave. The triangular wave structure is constructed of extensible links connected through flexible bending elements at each joint. Where, the links represent the unfolded sheet, and bending spring at each link-joint represents the lumped bending stiffness of a fold. Similar approximations have been made before for the other folded structures [3,24,30]. Apart from analytical simplicity, the triangular wave approximation yields a reasonable estimate of the wave contour length, when compared to the more sophisticated approximation of a sinusoidal shape. For commercial tissue papers $A_0/\lambda_0 \approx 0.1$, for such ratio it can be shown that the error between triangular and sinusoidal approximations lies within 1% (see Appendix B). Note that the crepe structure parameters such as λ_0 and A_0 represent the initial geometry of an unstretched creped tissue. Based on crepe wavelength and waveheight, the initial link-length (l_0) and semi-interlink angle (θ_0) can be derived as:

$$l_0 = \sqrt{\frac{\lambda_0^2}{16} + \frac{A_0^2}{4}}, \text{ and}$$

$$\sin \theta_0 = \frac{\lambda_0}{4l_0}.$$

(2)

Using equation 1, Crepe-Index (CI) for a triangular wave can be written as $CI = (4l_0/\lambda_0) - 1$. Which can be simplified using equation 2 as:

$$CI = \sqrt{1 + 4\frac{A_0^2}{\lambda_0^2}} = \frac{1}{\sin \theta_0} - 1.$$

(3)

Thus, higher Crepe Index is associated with folds of higher amplitude but smaller wavelength, or simply lower interlink angle. The same is also observed in experimental images shown in Figure 3(a).

A bilinear elastoplastic constitutive model has been used for the links with primary and secondary stiffness denoted by E_1, and E_2 respectively (Figure 4(b)). Such a relation has been shown to be adequate for fibrous structures [31, 32]. Note that E_1, and E_2 represents the slope of force/widthstrain ($f_w - \varepsilon$) curve, thus have a unit of N/m. The stiffness of elastoplastic bending springs can be derived as $k_\theta = Ewt^2/12l$, where w is the sheet's width, t is the unfolded sheet thickness, and E is the sheet's stiffnesss (E_1 or E_2 depending on the strain in sheet) in N/m [33]. Note that E represents the stiffness of sheet material after creping, thus should not be
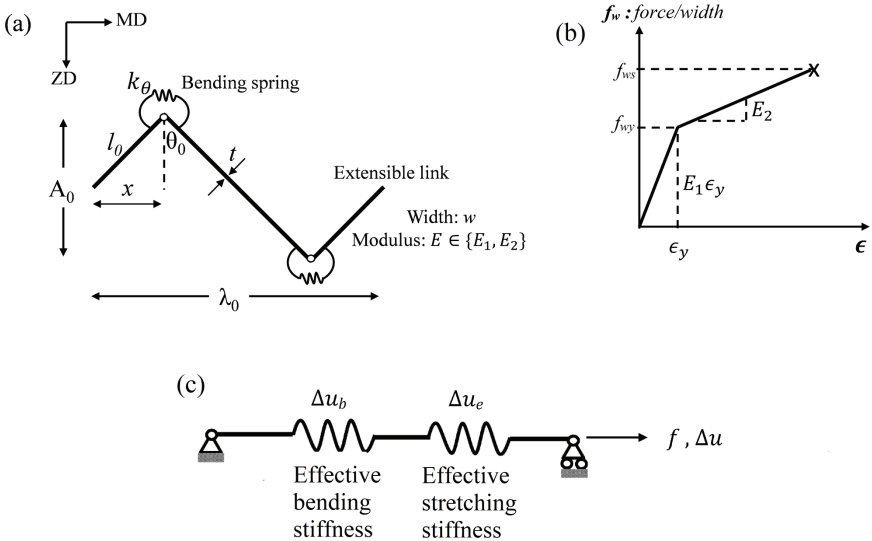
Figure 4. (a) Series link model for creped sheet, quantities with subscript $_0$ represents their initial values; (b) A bi-linear elastoplastic constitutive model used for sheet material. The ordinate represents the tensile force per unit width ($f_w = f/w$). The failure point under tension is represented by ×. (c) Creped sheet represented as a series combination of stiffness due to bending and stretching, as suggested by equation 4.

confused with the stiffness of uncreped sheet (sheet before creping). The difference between E and uncreped sheet stiffness arises due to de-densification during creping process, which is not considered in the present study.

If l and θ represent the link-length and semi-interlink angle at any instant, the instantaneous wavelength $\lambda = 4l/\sin\theta$. The instantaneous elemental change in wavelength will give the total elemental deformation (Δu) of the structure. Therefore:

$$\Delta u = \Delta\lambda = 4\Delta l/\sin\theta + 4l\Delta\theta \cos\theta. \tag{4}$$

The first term in equation 4 can be interpreted as displacement due to link stretching ($\Delta u_e = 4\Delta l/\sin\theta$), while second term as displacement due to fold bending ($\Delta u_b = 4l\Delta\theta \cos\theta$). Thus, as shown in Figure 4(c), the total elemental deformation (Δu) of the structure is the sum of elemental deformations in stretching and bending modes. Note that the equation 4 does not have a term coupling the two deformation modes. The above mode-decoupling is because of the simplistic assumption of crepe structure as a triangular wave of extensible but unbendable

links, with bending stiffness lumped at joints. Thus with the above assumption, the crepe structure can be conceptualized as a series combination of stiffnesses due to stretching and bending modes, as shown in Figure 4(c). The stiffness of stretching mode is proportional to Ew/l, while that of bending is proportional to $Ewt^2/12l^3$. The bending to stretching stiffness ratio is thus proportional to the slenderness ratio $(t/l)^2$, which is less than one for real crepes. Thus, bending is a softer mode of deformation. Thus under a tensile load, more energy is stored in the less stiff, bending mode.

3.1.1 Solution Method

We solve for displacement by applying a force f on one wavelength of the creped sheet in incremental steps. The principle of stationary potential is applied for every incremental step [34], thus at the i_{th} step, the incremental change in the total potential $\Delta\Pi_i$ can be written as:

$$\Delta\Pi_i = \Delta U_{e,i} + \Delta U_{b,i} - f_i \Delta u_i = 0, \tag{5}$$

where $\Delta U_{e,i}$ and $\Delta U_{b,i}$ are changes in stretching and bending strain energies at the ith step. Using the series-spring argument, the total incremental displacement at step i can be expanded as sum of instantaneous incremental displacements due to stretching and bending modes, i.e, $\Delta u_i = \Delta u_{e,i} + \Delta u_{b,i}$. The applied instantaneous force can be written in terms of loading history as $f_i = f_{i-1} + \Delta f_i$. The The link tension and bending spring moment at i^{th} step is updated as $T_i = f_i \sin\theta_{i-1}$ and $M_i = f_i l_{i-1} \cos\theta_{i-1}$. Using continuum relations, the change in stretching and bending strain energies at i^{th} step can be derived as $\Delta U_{e,i} = 4l_{i-1} \sin^2 \theta_{i-1} f_i \Delta f_i/(Ew)$ and $\Delta U_{b,i} = 2 f_i l_{i-1}^2 \cos^2\theta_{i-1}\Delta f_i/k_{\theta,i-1}$. Where bending stiffness at $i-1$ step is given by $k_{\theta,i-1} = Ewt^2/12l_{i-1}$. Using the series-spring argument, incremental displacement in each mode can be written as: $\Delta u_{e,i} = \Delta U_{e,i}/f_i$ and $\Delta u_{b,i} = \Delta U_{b,i}/f_i$. Thus:

$$\Delta u_{e,i} = \frac{4l_{i-1} \sin^2 \theta_{i-1}}{Ew} \Delta f_i, \text{ and}$$
$$\Delta u_{b,i} = \frac{2l_{i-1}^2 \cos^2 \theta_{i-1}}{k_{\theta,i-1}} \Delta f_i. \tag{6}$$

Using equation 4, incremental displacement at i^{th} step in stretching and bending modes can be written as: $\Delta u_{e,i} = 4\sin\theta_{i-1}\Delta l_i$ and $\Delta u_{b,i} = 4l_{i-1}\cos\theta_{i-1}\Delta\theta_i$, respectively. Therefore, the incremental change in link-length and semi-interlink angle at i^{th} step can now be expressed as:

$$\Delta l_i = \frac{l_{i-1} \sin \theta_{i-1}}{Ew} \Delta f_i, \text{ and}$$

$$\Delta \theta_i = \frac{l_{i-1} \cos \theta_{i-1}}{2k_{\theta,i-1}} \Delta f_i. \tag{7}$$

As we now know the incremental change in link-length and semi inter-link angle at step i, their total values can be calculated as: $l_i = l_{i-1} + \Delta l_i$ and $\theta_i = \theta_{i-1} + \Delta \theta_i$. The instantaneous wave height and wavelength of the structure can be calculated from instantaneous link length and semi inter-link angle as: $A_i = 2l_i \cos \theta_i$, and $\lambda_i = 4l_i \sin \theta_i$. Thus, the total incremental displacement can be found for a given incremental force, updating the changes in link-length and inter-link angle at each step. A load-displacement (f–u) curve for the creped sheet follows from the above analysis. The force/width and strains can be found as $f_{wi} = f_i/w$, and $\varepsilon_i = u_i/\lambda_0$.

3.1.2 Yielding and Failure Criteria

Yielding in the stretching mode is based on the elastoplastic constitutive model (Figure 4 (b)), i.e. if the strain in the link is less than the yield strain (ε_Y), the link stiffness is E_1, otherwise it is E_2. For bending springs, the force required for yielding is derived using flexure fomula for Euler-Bernoulli beam as $f_y = wtE_1\varepsilon_Y/(6lcos\theta)$ [24, 33]. For the applied force $f \leq f_Y$, the bending stiffness $k_\theta = E_1wt^2/12l$, while for $f > f_Y$, $k_\theta = E_2wt^2/12l$. Since, the bending stiffness of folds is dependent on sheet stiffness, if axial springs yield prior bending springs, bending springs are also assumed to be yielded.

In the tensile test of a real tissue paper, the tissue strength depends on mechanisms such as interfibre bond rupture, strain localization, and non-affine deformation [18, 21, 35, 36]. Since the above mechanisms are not considered in our study, the tensile test ends when the maximum force/width in the sheet reaches the specified value (f_{ws}), the corresponding value of strain is taken as stretch.

3.2 Model Results

The above incremental displacement methodology is employed as a MATLAB program. The relevant parameters and their definitions are summarized in Table 1. Parameter values are informed from previous experimental and numerical studies [14,18,21,25]. We will first present the model results explaining nonlinear evolution of the tensile response of the tissue. Later, the effect of Crepe Index on stretch and initial stiffness is discussed in detail.

Table 1. Parameter definitions and their default values [14,18,21,25]

Parameter	Notation	Default values	Units
Primary sheet stiffness	E_1	3	kN/m
Secondary sheet stiffness	E_2	0.3	kN/m
Strain to yield	ε_Y	2%	
Tensile strength of creped sheet	f_{ws}	50	N/m
Sheet thickness	t	30	μm
Initial wavelength	λ_0	230	μm

3.2.1 Tensile Response Evolution

Figure 5 shows the tensile response of the idealized triangular fold tissue paper. In Figure 5 (a), the secondary stiffness of sheet (E_2) is varied while maintaining a constant primary sheet stiffness (E_1). For a linearly elastic material ($E_2/E_1 = 1$), the tensile curve shows a moderate geometric nonlinearity (a slightly increasing stiffness) owing to the crepe structure. However, for the elastoplastic case, an inflection is seen in the tensile curve due to yielding in link and bending springs. Note that the responses before yielding are identical since E_2/E_1 is varied by changing E_2 only. As E_2/E_1 decreases, the response becomes softer after the inflection. Note that, unlike experiments (Figure 3(b)), the inflection from DEM is not gradual; this is due to the discrete nature of the model, collapsing the CD information onto a single curve, and the presence of a single wavelength.

Solid curves in Figure 5(b) summarize the DEM results about the influence of CI on the tensile response of the creped sheet. The CI values for commercial tissues lie within 10−20%, however for more comprehensive understanding we vary the CI from 2% to 20%. As CI decreases the tensile response becomes stiffer. At very low values of CI (e.g. 2%), link stretching is the dominant deformation mode, thus the response converges to the constitutive elastoplastic tensile response of the flat sheet (qualitatively compare *CI*= 2% curve in Figure 5(b) with constitutive law in Figure 4(b)). In contrast, at higher CI, the initial stiffness of the creped sheet decreases due to the dominating bending mode (less stiff mode of deformation). At higher strain, when the structure almost *unfolds*, stretching dominates, and creped sheet stiffness approaches the secondary stiffness of sheet (E_2), therefore, all responses of discrete elastoplastic model (DEM) in Figure 5(b) approach the same slope near failure. Thus, the DEM tensile response captures the initial stiffness, inflection, and re-stiffening as also observed in the experimental tensile response shown in Figure 1(d).

The DEM results are also compared with Vandenberghe's inextensible bending model (IBM) [24] in Figure 5(b). Although both model show same initial stiffness for CI values for commercial tissues (10−20%), IBM differs with DEM on
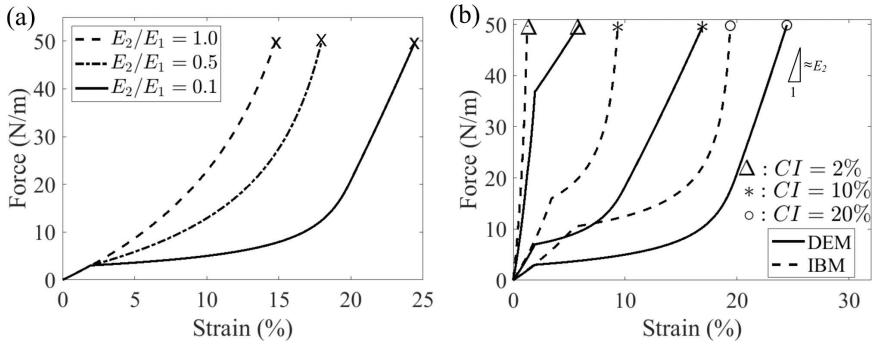
Figure 5. Effect of material and geometric non-linearity on the tensile response of creped tissue: (a) Tensile curve using discrete elastoplastic model (DEM) for different E_2/E_1 ratio at CI=20%. Ratio is varied by changing the value of E_2. The failure point is represented by ×; (b) Tensile curves for different CI (shown by different failure point symbols). DEM (solid curve) results are also compared with inextensible bending model (IBM, shown by dashed curve) by Vandenberghe et al. [24].

two key aspects: first, the slope near failure in IBM approaches infinity (singularity), while with DEM it approaches the secondary stiffness E_2. Thus, due to rapid stiffening, IBM predicts a lower failure strain (or stretch) for the same sheet strength. Approaching singularity is the reason why IBM show a higher stiffness at low CI of 1% in Figure 5(b). Second, due to the absence of link flexibility, the inflection in IBM is governed by the yielding in bending springs only. While in DEM, link springs yield first, which cause the bending springs to yield, due to the dependence of bending stiffness on the sheet stiffness ($k_\theta = Ewt^2/12l$, where $E \in \{E_1, E_2\}$). Thus, as compared to IBM, discrete elastoplastic model (DEM) is a more suitable to comprehensively understand nonlinear evolution of tensile response of tissue.

The above DEM results suggest that the nonlinearity in tensile response for a creped sheet is due to both material as well as geometric nonlinearity. The former is responsible for the inflection in the tensile response, while the latter is responsible for overall softening of response due to increased dominance of bending (less stiff) mode.

3.2.2 *Effect of Crepe Index on Stretch and Initial Stiffness*

Figure 6 summarizes the effect of CI on the stretch and initial stiffness. Figure 6(a) shows that for very low CI (< 0.5%, or almost flat sheet), the stretch has a minimal dependence on CI (almost zero slope), therefore stretch values are dominated by link-stretching. For CI above 5%, contribution from bending springs

dominates and stretch shows a linear correlation with CI, which is in agreement with experimental results shown in Figure 3(a). From equation 3, it can be inferred that higher CI is associated with folds of higher frequency and waveheight. Thus, the creped sheet with higher CI will undergo more unfolding, thus increasing the failure strain (stretch). Also, a slight reduction in stretch with increasing sheet thickness to crepe wavelength ratio (or t/λ_0) is observed. For instance, at CI=10%, when t/λ_0 is increased by 200% (0.05−0.15), stretch decreases by just 40%. The above dependence can be explained by increased bending stiffness at higher t/λ_0, thus reducing the failure strain for a given sheet strength. Although for commercial tissues the value of t/λ_0 lies within 0.1−0.15, the range is exaggerated in numerical study (0.05−0.15) to understand the effect of t/λ_0 over a larger range. The results in Figure 6(a) are compared with $y = x$ line, which represents the geometry argument as mentioned in section 2.1, i.e, stretch will be same as CI in case of inextensible unfolding (i.e, no change in total length of the sheet). The region above $y = x$ line represents the case when sheet failure occurs post unfolding, and vice-versa. In the linear region, the average slope of the stretch-CI lines shown in Figure 6(a) is 0.9, which is almost same as the experimental observation. It can be seen from the plots that the slopes of all of the curves is approaching to that of $y = x$ line (i.e, 1). This confirms the experimental observation that the total stretch is a sum of Crepe Index and strain due to sheet stretching. The difference between total stretch and CI is dependent on parameters such as t/λ_0 and sheet stiffness. The stretch of uncreped sheets is of the order of 2%, while CI of the creped sheets is above 15 %, thus the overall stretch of the creped tissue is governed by CI. Thus, the slight variability of stretch with t/λ_0 and low base sheet stretch can be used as the facts to explain the good correlation between experimental stretch and CI values (Figure 3(b)), despite the variability in furnish and machine conditions. Another interesting observation is that the flat sheet stretch (stretch at zero CI in Figure 6(a)) is lower than the intercept of stretch-CI line in the linear region (CI>10%). The jump can be explained by transition of deformation-mode from stretching to bending. Thus, intercept of the fitted stretch-CI line (stretch at CI=0) based on the data in the linear region (CI>10%) does not represent the stretch of the flat sheet.

To study the influence of CI on the initial stiffness (E_0), we first compare our model results with inextensible bending model (IBM) by Vangenberghe et al. [24]. Based on IBM assumption of link inextensibility, we derive the following analytical expression relating initial stiffness E_0 of creped sheet with t/λ_0, CI, and primary sheet stiffness E_1 (see Appendix C for complete derivation) as:

$$E_0 = \frac{8}{3} E_1 \left(\frac{t}{\lambda_0}\right)^2 \frac{1}{CI(1+CI)(2+CI)}. \tag{8}$$

Equation 8 is compared with the discrete elastoplastic model (DEM) in Figure 6(b). To non dimensionalize, a ratio of E_0/E_1 and $(t/\lambda_0)^2$ is plotted. Due to approaching singularity at low CI values IBM overestimates the initial stiffness, as also observed in Figure 5(b). The analytical results lie in close agreement with the model for higher values of CI in the practical range (CI> 10%). In Figure 6(b) DEM and IBM results are also compared with single layer 1D particle dynamics creping model by Pan et al. [14]. In 1D particle dynamics model, an elastoplastic sheet is crepe at a speed of 30 m/s, CI is controlled by varying CR and adhesive toughness, rest of the parameters are same as mentioned in Table 1. For CI> 10%, a very good agreement is seen among all three models. The above agreement suggests that for higher CI values (> 10%), equation 8 is suitable for initial stiffness estimation, however, for lower CI, DEM is more suitable (as compared to IBM) due to consideration of stretching effects.

Figure 6(c) shows the influence of CI on the initial stiffness of crepe structure using DEM. Note that the initial stiffness (E_0) is non-dimensionalized with respect to primary stiffness of the sheet (E_1). At zero CI (or perfectly straight web) the initial stiffness of creped sheet is exactly equal to the primary sheet stiffness (E_1). As CI increases, the bending stiffness k_θ reduces due to increment in link-length l_0, thus decreasing the overall stiffness of the creped sheet.

Beside dependence on CI and primary sheet stiffness (E_1), the initial stiffness shows a significant increase with t/λ_0, as observed in Figure 6(c). For instance, at CI=10%, when t/λ_0 is increased by 200% (0.05−0.15), E_0/E_1 increases by 650%. The dependence of E_0 on t/λ_0 can again be explained by increased bending stiffness. Analytical expression in equation 8 suggests a quadratic dependence of E_0/E_1 on t/λ_0 ratio, which is also observed from DEM results when plotted on log-log scale in Figure 6(d).

As manifested in Figure 6(c), the dependence of initial stiffness of creped sheet on t/λ_0 and primary stiffness of the sheet material (E_1) can be used to explain the observed unclear correlation of measured initial stiffness and CI (Figure 3(c)). From Table A.1, it can be seen that although grades A and B have same furnish, t/λ_0 for B is 33.3% higher than that of grade A. Also, the true values of primary sheet stiffness (E_1) after creping is not known. The measurement of E_1 on a high speed tissue machine is challenging, as it depends on uncreped sheet thickness and de-densification while creping. Similarly, for other grades, the variability in t/λ_0 and sheet stiffness can be a reason for the unclear correlation between initial stiffness and CI in experimental results. However, for quantitative comparison of DEM stretch values with experiments, E_1 values are predicted using DEM through error minimization of the function $|E_0^{(DEM)} - E_0^{(exp)}|$, based on the measured values of CI, crepe wavelength, initial stiffness $E_0^{(exp)}$, and t/λ_0. The estimated primary stiffness values vary between 1.5 kN/m - 3.5 kN/m for all six grades, which is a significant variation, thus may be one source of unclear correlation for initial stiff-
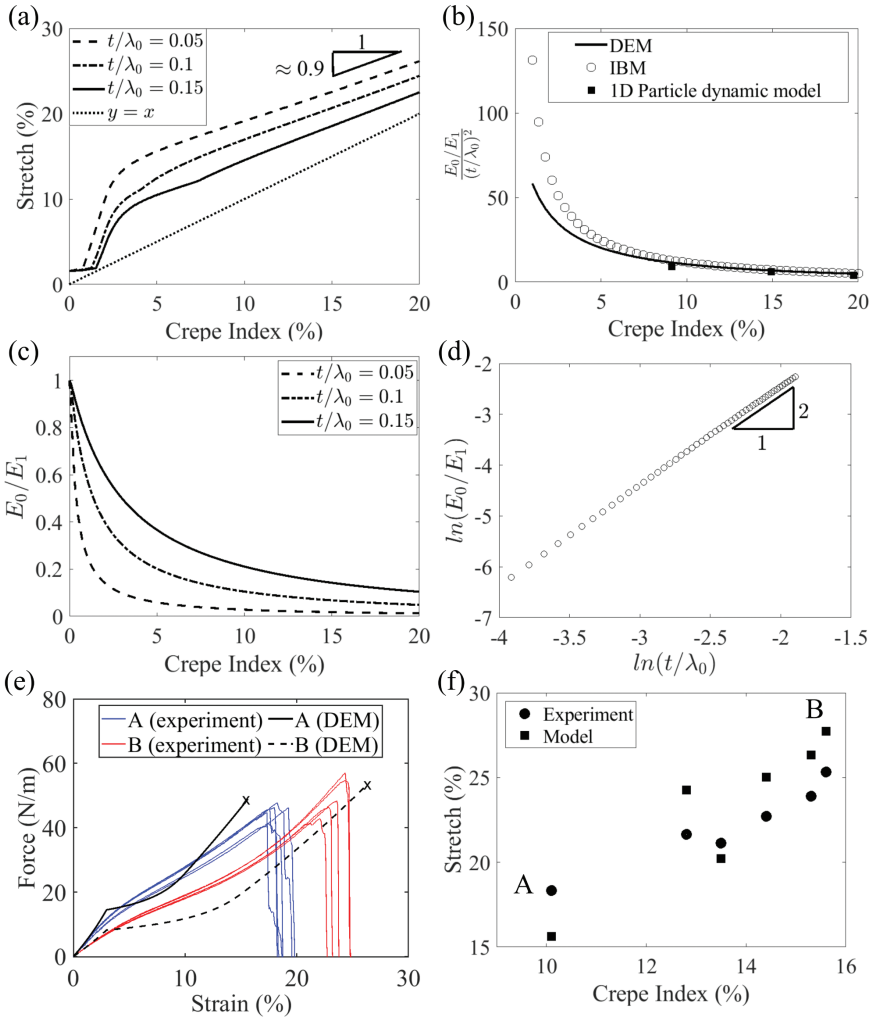
Figure 6. (a) Effect of Crepe Index on stretch using discrete elastoplastic model (DEM); (b) Comparison of DEM with analytical relation (equation 8) derived for inextensible bending model (IBM). To non-dimensionalize, a ratio of E_0/E_1 and $(t/\lambda_0)^2$ is plotted; (c) Effect of Crepe Index on initial stiffness from DEM; (d) Power law scaling using DEM for initial stiffness ratio E_0/E_1 with t/λ_0, note that the same power-law is predicted by equation 8; (e) Tensile response comparison between model and experiments for grades A and B shown in figure 3; (f) Comparison of mean stretch values from DEM and measurements.

ness with Crepe Index. Now, using the predicted E_1 values, and the measured strength, we estimate the DEM tensile response for commercial grades. The estimated tensile response for grades A and B is shown in Figure 6(e). Since unknown, E_2/E_1 and yield strain are assumed to be 0.1 and 2% respectively. The DEM tensile responses show that the qualitatively same behaviour. However, the experimental response is more gradual, which can be due to the fact that the actual crepe structure consists of a spectrum of folds of different wavelengths, however the model consists a fold of dominant wavelength and amplitude. The DEM estimated stretch values for all six grades are compared with true values in Figure 6(f). The DEM predicted stretch-CI variation is in qualitative agreement with measurements. The discrepancy in values can be due to uncertainty in E_2/E_1, yield strain values, and the presence of fold spectrum instead of single wavelength fold, as approximated in the model.

4 CONCLUSION

Creped tissue paper is a low-density fiber network with micro folds imparted by interaction with the creping blade. Parameters like Crepe Ratio (CR) and Crepe Frequency (CF) are virtually uncorrelated with important tissue tensile properties such as stretch and initial stiffness. We propose a parameter called Crepe Index (CI) that quantifies the degree of folding in a creped tissue paper. The CI for a variety of commercial tissue grades is measured from edge images. Though superficially similar to the CR, experimental data show that both CI and CR are different quantities. Tensile tests show that CI has a direct correlation with stretch, but an unclear correlation with initial stiffness.

Through a discrete elastoplastic model (DEM), we explain the tensile curve nonlinearity, dependence of stretch on CI, and possible reasons for inconclusive correlation of measured initial stiffness with CI. The tissue paper is modelled as a triangular wave of extensible links, connected through bending springs. A bilinear elastoplastic constitutive model is used for the sheet material. The model shows that both material and geometric nonlinearity are responsible for the nonlinear evolution of tensile response. The former is responsible for the inflection in tensile response. The latter is responsible for reduced initial stiffness as compared to the flat sheet, due to contribution from the bending deformation mode.

Using DEM, we study the dependence of stretch and initial stiffness on CI. At very low CI, the network stretching dominates and the failure strain shows little dependence on CI. At high CI values, bending effects are dominant and the strain to failure is a linear function of CI. The linear correlation of stretch with CI from DEM agrees with experiments. It is also observed from both experiments and model results that for CI range of tested commercial tissues, the stretch shows linear dependence on CI

with a slope ≈ 1, and stretch values are higher than CI (positive intercept). Thus, the stretch of creped tissue is a combination of the crepe unfolding (Crepe Index effects) and strain due to network stretching. The good experimental correlation between CI and stretch despite of variability in furnish and machine conditions is explained by a feeble dependence of stretch on t/λ_0, and relatively lower values of base sheet stretch ($\sim$ 2%) as compared to CI values ($\sim$ 15%), thus, CI governing the stretch.

DEM results shows that the initial stiffness varies inversely with CI due to increased contribution from the bending mode at high CI. Assuming inextensible bending (IBM), an analytical expression relating initial stiffness with CI and sheet properties is derived. The predicted initial stiffness with DEM and IBM are in good agreement with 1D particle dynamics model for CI of real tissues (> 10%). The agreement suggests that for the high CI range (CI> 10%), IBM is reasonable for initial stiffness prediction, however for lower CI values, DEM is more appropriate as compared to IBM due to consideration of stretching effects. Apart from dependence on primary sheet stiffness and CI, initial stiffness shows a quadratic dependence of initial stiffness with the thickness to initial wavelength ratio (t/λ_0). The experimental data shows a variability in t/λ_0, and true values of E_1 and E_2 are unknown due to measurement limitations. Therefore, the variability in t/λ_0 and primary stiffness of sheet material (E_1) can be possible reasons for the unclear correlation of experimentally measured initial stiffness of creped sheet with CI. Hence, a systematic experimental study is required in future to study the effect of CI on the initial stiffness and compare it with the proposed theoretical model.

The fact that tissue papers are low-density, bonded fibre network structures makes them discrete structures. Deformation of such structures is non-affine and can have complexities due to progressive damage, de-densification, strain localization, and wiremark effects, which are not considered in the presented model. As pointed out earlier, the estimation of true value of primary sheet stiffness (E_1) required the information about de-densification while creping. Also, it has been observed by Srivastava that differences in wiremark and crepe structure are related to stretch of a creped tissue [25]. Addressing the effects of de-densification, wiremark, and fibre properties require the microscale modelling of tissue structures, which is planned for future research.

ACKNOWLEDGEMENT

REFERENCES

[1] T. De Assis, Fundamental evaluation of the impact of cellulosic fiber features and manufacturing technologies on the performance and value of tissue paper products, Ph.D. thesis, North Carolina State University (2019).

[2] H. Hollmark, Study of the creping process on an experimental paper machine, *STFImeddelande, Series B* (1972) 144.

[3] W. McConnel, The science of creping, Tissue World Americas (2004).

[4] K. Pan, A. Srikantha Phani and S. Green, Particle dynamics modeling of the creping process in tissue making, *Journal of Manufacturing Science and Engineering, Transactions of the ASME* 140 (7) (2018). doi:10.1115/1.4039649.

[5] H. C. Schniepp, K. N. Kudin, J.-L. Li, R. K. Prud'homme, R. Car, D. A. Saville and I. A. Aksay, Bending properties of single functionalized graphene sheets probed by atomic force microscopy, *ACS Nano* 2 (12) (2008) 2577–2584.

[6] S. Cranford, D. Sen and M. J. Buehler, Meso-origami: folding multilayer graphene sheets, *Applied Physics Letters* 95 (12) (2009) 123121.

[7] H. Kobayashi, B. Kresling and J. F. Vincent, The geometry of unfolding tree leaves, *Proceedings of the Royal Society of London. Series B: Biological Sciences* 265 (1391) (1998) 147–154.

[8] A. Goriely and M. Tabor, Spontaneous helix hand reversal and tendril perversion in climbing plants, *Physical Review Letters* 80 (7) (1998) 1564.

[9] A. Lebee, From folds to structures, a review, *International Journal of Space Structures* 30 (2) (2015) 55–74.

[10] K. Bertoldi, V. Vitelli, J. Christensen and M. Van Hecke, Flexible mechanical metamaterials, *Nature Reviews Materials* 2 (11) (2017) 1–11.

[11] M. Ramasubramanian, Physical and mechanical properties of towel and tissue, in: *Handbook of Physical Testing of Paper*, CRC Press, 2001, pp. 683–896.

[12] J. P. Raunio and R. Ritala, Simulation of creping pattern in tissue paper, *Nordic Pulp & Paper Research Journal* 27 (2) (2012) 375–381.

[13] T. de Assis, J. Pawlak, L. Pal, H. Jameel, L. W. Reisinger, D. Kavalew, C. Campbell, L. Pawlowska and R. W. Gonzalez, Comparison between uncreped and creped handsheets on tissue paper properties using a creping simulator unit, *Cellulose* 27 (10) (2020) 5981–5999.

[14] K. Pan, R. Das, A. S. Phani and S. Green, An elastoplastic creping model for tissue manufacturing, *International Journal of Solids and Structures* 165 (2019) 23–33.

[15] D. Page and R. Seth, The elastic modulus of paper: The importance of fiber modulus, bonding and fiber length, *TAPPI 63* (6) (1980) 113–116.

[16] H. Cox, The elasticity and strength of paper and other fibrous materials, *British journal of Applied Physics* 3 (3) (1952) 72.

[17] S. B. Lindstrom and T. Uesaka, Particle-level simulation of forming of the fiber network in paper making, *International Journal of Engineering Science* 46 (9) (2008) 858–876.

[18] S. Borodulina, A. Kulachenko, S. Galland and M. Nygards, Stress-strain curve of paper revisited, *Nordic Pulp and Paper Research Journal* 27 (2) (2012) 318–328.

[19] P. Bergstrom, S. Hossain and T. Uesaka, Scaling behaviour of strength of 3d-, semi-flexible-, cross-linked fibre network, *International Journal of Solids and Structures* 166 (2019) 68–74.

[20] M. Islam and R. Picu, Effect of network architecture on the mechanical behavior of random fiber networks, *Journal of Applied Mechanics* 85 (8) (2018).

[21] R. Das, K. Pan, S. Green and A. S. Phani, Creped tissue paper: A microarchitected fibrous network, *Advanced Engineering Materials* (2020) 2000777.

[22] R. Das, Experimental studies on creping and its influence on mechanical properties of tissue paper products, Master's thesis, University of British Columbia (2019).

[23] K. Pan, Modeling the creping process in tissue making, Ph.D. thesis, University of British Columbia (2019).

[24] N. Vandenberghe, E. Villermaux, A brittle material with tunable elasticity: Crepe paper, *Comptes Rendus Mecanique* 347 (4) (2019) 382–388.

[25] P. Srivastava, Experimental characterization of tissue structure and the impact of forming fabric on tissue properties, Master's thesis, University of British Columbia (2021).

[26] P. Sutton, C. Joss, and B. Crossely, Factors affecting fiber characteristics in pulp, in: *Pulping Process and Product Quality Conference Proceedings*, 2000.

[27] N. Epstein, On tortuosity and the tortuosity factor in flow and diffusion through porous media, *Chemical Engineering Science* 44 (3) (1989) 777–779.

[28] T. U. Kaempfer, M. Schneebeli and S. Sokratov, A microstructural approach to model heat transfer in snow, *Geophysical Research Letters* 32 (21) (2005).

[29] Tissue paper and tissue products – Part 4: Determination of tensile strength, stretch at maximum force and tensile energy absorption, Standard, International Organization for Standardization, Geneva, Switzerland (2016).

[30] F. Lechenault, B. Thiria and M. Adda-Bedia, Mechanical response of a creased sheet, *Physical Review Letters* 112 (24) (2014) 244301.

[31] M. Ramasubramanian and Y. Wang, A computational micromechanics constitutive model for the unloading behavior of paper, *International Journal of Solids and Structures* 44 (22-23) (2007) 7615–7632.

[32] D. Wilbrink, L. Beex and R. Peerlings, A discrete network model for bond failure and frictional sliding in fibrous materials, *International journal of Solids and Structures* 50 (9) (2013) 1354–1363.

[33] S. P. Timoshenko, *Strength of Materials Part 1: Elementary Theory and Problems*, 3rd Edition, Van Nostrand Co., Inc., Princeton, 1955.

[34] R. D. Cook, et al., *Concepts and Applications of Finite Element Analysis*, 4th Edition, John wiley & sons, 2007.

[35] S. Deogekar, R. Picu, On the strength of random fiber networks, *Journal of the Mechanics and Physics of Solids* 116 (2018) 1–16.

[36] C. R. Picu, Mechanics of random fiber networks: Structure–properties relation, in: *Mechanics of Fibrous Materials and Applications*, Springer, 2020, pp. 1–61.

[37] R. Bulirsch, Numerical calculation of elliptic integrals and elliptic functions, *Numerische Mathematik* 7 (1) (1965) 78–90.

APPENDICES

Appendix A: Experimental Data

Table A.1. Relevant parameters for grades A and B shown in Figure 3. A and B share the same furnish. Mean and standard error for stretch, initial stiffness, and t/λ_0 are reported.

Grades	Grammage (g/m²)	Crepe Index (%)	Crepe Ratio (%)	Crepe Frequency (folds/m)	Stretch (%)	Initial stiffness (kN/m)	t/λ_0
A	14.3	10.1±0.6	22.66	4015.75	18.32±0.64	0.79±0.021	0.12±0.016
B	20.1	15.3±0.7	21.07	3267.72	23.89±0.28	0.48±0.007	0.16±0.011

Appendix B: Contour Length Comparison between Triangular and Sine-wave Approximation

In this section we are going to compare the contour length of sine and triangular wave. For a wavelength λ_0, and wave height A_0, contour length over one wavelength for triangular and sinusoidal wave can be written as:

$$l_c^{(tri)} = 4\sqrt{\frac{A_0^2}{4} + \frac{\lambda_0^2}{16}}, \text{ and}$$

$$l_c^{(sin)} = \int_0^{\lambda_0} \sqrt{1 + \left(\frac{A_0}{\lambda_0}\right)^2 \cos^2\left(\frac{2\pi x}{\lambda_0}\right)}\, dx. \tag{B.1}$$
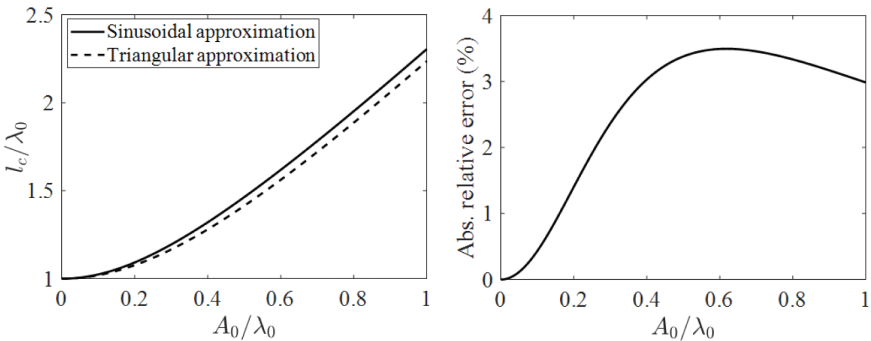

Figure 7. Contour length of wave with height A_0 and wavelength λ_0 over one wavelength for triangular and sinusoidal approximation. Note that the maximum relative error between both is 3.49%, thus triangular approximation is reasonable for contour length estimation.

Contour integral for sinusoidal wave can be calculated exactly using elliptic integral of second kind [37]. Non-dimensionalized contour length (l_c/λ_0) using both approximations, and the absolute relative error ($|l_c^{tri} - l_c^{sin}|/l_c^{sin}$) are compared in Figure 7. For tissue papers the ratio $A_0/\lambda_0 \sim 0.1$, thus the error between triangular and sinusoidal approximations lie within 1%.

Appendix C: Analytical Expression for the Initial Stiffness of Creped Sheet

Under the assumption that the link length doesn't undergo any change (inextensible bending), the bending moment at any instant can be written as $M = fl_0 \cos\theta$. Bending moment can also be expressed in terms of bending spring coefficient and inter-link angle as: $M = k_\theta(2\theta - 2\theta_0)$, where 2θ is the inter-link angle at any instant, while $2\theta_0$ is the initial inter-link angle. Thus applied force can be written as:

$$f = \frac{2k_\theta(\theta - \theta_0)}{l_0 \cos\theta},$$

(C.1)

where $k_\theta = E_1 w t^2/12l_0$. The link-length can be written in terms of Crepe Index and initial wavelength as $l_0 = \lambda_0(1 + CI)$. As shown in Figure 4(a), horizontal component of each link can be written as: $x = l_0 \sin\theta$ and $x = x_0(1 + \varepsilon)$, where ε is the strain in the direction of applied force. stiffness at any instant in the elastic limit can be derived as:

$$E = \frac{1}{w}\frac{\partial f}{\partial \theta}\frac{\partial \theta}{\partial \varepsilon} = \frac{2k_\theta x_0}{w l_0^2 \cos^2\theta}[1 + (\theta - \theta_0)\tan\theta].$$

(C.2)

Using the initial configuration at $\varepsilon = 0$, initial stiffness ratio of the creped sheet can be found as:

$$\frac{E_0}{E_1} = \frac{8}{3}\left(\frac{t}{\lambda_0}\right)^2 \frac{1}{CI(1 + CI)(2 + CI)}.$$

(C.3)

INFLUENCE OF CREPE STRUCTURE ON TENSILE PROPERTIES OF TISSUE PAPER

Shubham Agarwal, *Prabhat Srivastava,*
Sheldon I. Green and A. Srikantha Phani

Department of Mechanical Engineering, The University of British Columbia, Vancouver, Canada

Artem Kulachenko   Royal Institute of Technology (KTH)

When you evaluate the contribution of the bending stiffness and the elongational stiffness, you base both of them on the same elastic modulus. In other words, you assume that you can derive the bending stiffness from the elastic modulus and thickness of the paper. However, the creping process itself induces damage to the structure and therefore the relationship between the bending stiffness, elastic modulus and thickness is no longer ensured owing to delamination in the sheet structure. Do you have plans to account for that? I think this would be a way to at least explain the differences that you see between the numerical and the experimental predictions where the numerical prediction overshoots the measured stiffness?

Shubham Agarwal

That is a valid point. Our model is based on the bending stiffness evaluation using the thickness. Due to that reason, this model, I believe, is more applicable for bulk kind of deformation in which there is no, or there is a less, inter-fibre separation but for more de-densified sheets, the thickness value cannot be used directly from the experiments because porosity is involved. One extension for this work is to relate that de-densification of the sheet with this model.

Discussion

Artem Kulachenko

It is not only about densification, but also about delamination between the plies. Think about the bending stiffness in the case where the plies are completely separated and the one when the plies are fully connected. You will be having differences because of the interlaminar shear resistance and I think the interlaminar delamination increases with increased crepe ratio.

Shubham Agarwal

Yes, I agree with that.

Warren Batchelor   Monash University

So, you are using a single value of thickness; but surely your thickness in a creped sheet is highly variable and your thickness from bend to bend is significantly variable, so how do you account for that?

Shubham Agarwal

Yes. But for this modelling work, the aim was to explain the non-linearity of tensile response and to connect the crepe structure with the tensile properties, that is the reason why we use such a simple geometry and without complicating it much with thickness variation. So, that is the reason why this does not fit very well with the experimental data, but it does give some qualitative insights. But yes . . . if we want to compare one to one, this model has some limitations because of the reasons you suggested.

Jarmo Kouko   VTT Technical Research Centre of Finland Ltd

I have one comment and then one question. As you know the crepe ratio, then you basically can calculate the dimensional shrinkage of the web by that value. In this seminar, we have at the poster presentation described relation between shrinkage and elongation. So the question is: have you looked at the relation between the dimensional shrinkage done by the creping and the elongation?

Shubham Agarwal

We have not looked at shrinkage in this work, but yes the shrinkage will be dependent on crepe ratio, it is like how much the sheet is being compressed but in this model we do not consider that at all.

Bill Sampson   University of Manchester

Both your crepe index and the crepe ratio should really correspond to the change in grammage of an uncreped sheet to a creped sheet. The change in grammage gives a global and simple measure, whereas your crepe index is a local measure, so I was rather surprised that the crepe index correlates with the stretch but the crepe ratio does not. Can you comment on that?

Shubham Agarwal

Crepe ratio does not correlate with stretch?

Bill Sampson

You say in the paper that crepe ratio is not a useful measure. You could not get a correlation?

Shubham Agarwal

Yes, because crepe index is based on the structure which we get after the creping, so it will be a direct measure of the crepe but crepe ratio is before creping.

Bill Sampson

Crepe ratio gives the difference in speed, which should be same as a difference in grammage, which should be captured by the crepe index?

Shubham Agarwal

It should but the crepe ratio will induce some other parameters like shrinkage in the sheet because of the change in speed of the reel and Yankee. But the crepe ratio itself is a measure of the structure, it does not have that quantification of shrinkage, but yes if we are able to correlate some quantity based on crepe index as well as crepe ratio, we should see some correlation with the grammage or the density (and shrinkage).

Peter de Clerck   PaperTec Solutions Pte Ltd

Thank you. It was an interesting paper. You focused very strongly on the strength of the tissue paper. However, the most important strength aspect in converting tissue paper is the tensile energy absorption which is the area under the

Discussion

stress-strain curve. Have you looked at this aspect and have you related it to your crepe ratio and your crepe index?

Shubham Agarwal

So, for tensile energy absorption, one another important parameter is the strength of the sheet but in this model we don't model the rupture of the sheet itself, we give it to a specific strength. When it reaches that specific value, we terminate the tensile test but in order to model that energy absorption more realistically or more faithfully, we should have some damage model in our sheet. This is a part of the plan for us, so we are working on like a fibre network model which will take care of the damage evaluation during the tensile test and we can correlate with both crepe index and with the energy absorption which consists of both the strength as well as the stiffness of the sheet.

Peter de Clerck

Strength itself is not as important in tissue as the energy absorption, which is important as you go through the reeling process or when you are trying to peel a web off the Yankee. It affects the separation of the sheets when you go for perforation, it maintains the web as you pull it through the converting operation and the reeling (log roll) operation. The individual strength of the sheet is nowhere near as important as the final TEA in manufacturing operations.

Shubham Agarwal

We can look into it but right now we have not looked into.

Douglas Coffin   Miami University

Could you put your last slide with the comparison of experimental results. When I look at the results, it seems like the model overpredicts the structural stiffening quite a bit. Both A and B show this, and A does not really have any structural stiffening in the actual material. I think the approach you are taking is really good, this is the same way I would do it but what I am wondering is where you are putting the plasticity and the bending should have more plasticity. You can load, unload, and reload it and look at how much plastic deformation you are actually getting to really see if your model is capturing the plasticity. I am wondering if you have done any cyclic loading type of test and does your bending have plasticity in it?

Shubham Agarwal

Yes, bending has plasticity but we haven't done virtual cyclic tensile.

Douglas Coffin

I think that will be instructive because the reloading curves are much stiffer than what you see there and I think you are overplaying the structural stiffness?

Shubham Agarwal

Yes, thank you.

Steven Keller   Miami University

Bill Sampson brings up a very good point about the relationship between the crepe ratio and creping index. I think what you will find is that the difference between the two is the bulking of the structure. Because if you are bulking, you are not changing the centre surface and then if you measure grammage and you combine the two, you will have an indication of the delamination that is occurring.

Joel Pawlak   North Carolina State University

Question for you on the slide, since Doug brought it up, I figured I would ask. So, if I recall correctly A and B were both made from the same furnish, correct?

Shubham Agarwal

Yes.

Joel Pawlak

So, B has the higher crepe index and so if I was to do one of those experiments that Doug suggested and that say for B go to 10% strain and then release it and measured the crepe index again, would my crepe index change and how will that fit into your model if then you re-ran with a new crepe index?

Shubham Agarwal

Yes, so if we load it and then unload it and measure the crepe index, there will be difference because of the plastic deformation which happened.

Discussion

Joel Pawlak

Will that new data follow the line according to you model that you have suggested? So, in other words, if I move B to the same crepe index as A through that method, would sample B then follow A?

Shubham Agarwal

I have not looked into that, but yes we can.

Joel Pawlak

I think it would be an experiment you want to try.

Shubham Agarwal

Yes, thank you.